ECCOMAS Congress 2016
VII European Congress on Computational Methods in Applied Sciences and Engineering
M. Papadrakakis, V. Papadopoulos, G. Stefanou, V. Plevris (eds.)
Crete Island, Greece, 5–10 June 2016

MULTI-SCALE FINITE ELEMENT ANALYSIS OF GRAPHENE/POLYMER NANOCOMPOSITES: ELECTRICAL PERFORMANCE

Asimina Manta[1], Matthieu Gresil[1,2], and Constantinos Soutis[2]

[1] i-composites lab, School of Materials, University of Manchester, James Lighthill Building, Sackville Street, Manchester M13 9PL, United Kingdom.
e-mail: asimina.manta@postgrad.manchester.ac.uk

[2] Aerospace Research Institute, Faculty of Engineering and Physical Sciences, University of Manchester, James Lighthill Building, Sackville Street, Manchester M13 9PL, United Kingdom.
constantinos.soutis@manchester.ac.uk
matthieu.gresil@manchester.ac.uk

Keywords: Graphene, Finite Element Analysis, Electrical Conductivity, Nanocomposites, Computational methods

Abstract. *This paper presents a multi-scale, multi-physics finite element model (FEM) simulating the electrical performance of single layer graphene/insulator under DC loading, which would be easily applied to most cases, extended to a more sophisticated material architecture in respect of being scientifically structured and proven. The approach consists of the creation of a unit cell and a representative volume element (RVE) micro-scale nanocomposite model on a commercially available FE package. The implementation of these models has been considered satisfactory and successful, as the variation of nanocomposite's electrical conductivity in respect to the volume content was in accordance with experimental data. Moreover, the numerical simulation was in accordance with the classical percolation law predictions, while the obtained percolation thresholds in terms of aspect ratio obey the Excluded Volume Theory. The graphene shape was considered in the analysis as a geometric parameter, being proved that the shape does not exhibit any profound effect on the electrical performance of the graphene/insulator nanocomposite. Finally, this model is capable to predict the full percolation response of the nanocomposite and can be applied to any nanocomposite architecture in contrast to general theories that can only estimate the percolation threshold rather than the full response.*

1 INTRODUCTION

Conductive polymers have been extensively studied for their potential applications in light emitting devices, batteries, electromagnetic shielding, and piezoresistive sensors. At first, carbon black [1], [2], metallic powder [3–5], polyaniline [6] and graphite [7] were used as electrical reinforcement in polymer, but high concentration was necessary to achieve the percolation threshold which endangered the mechanical properties of the nanocomposites due to the formation of agglomerations. Later, several researchers proposed polymer nanocomposites reinforced with graphene nanoparticles and its derivatives (expanded graphite, graphene nanoplatelets, graphite oxide, functionalized graphene/expanded graphite), which are able to form more stable 3D conductive networks in lower volume content as a consequence of their high aspect ratio (AR-ratio of main particle dimension to minor one) [8–15].

However, despite the high financial and time cost of material preparation and experimental work, there are a few computational models predicting the electrical response of graphene/polymer nanocomposites. Most of them are based on molecular dynamics and geometrical programming routines, being able mainly to predict the percolation threshold of the nanocomposites with high computational cost. Oskouyi et al. [16] appeared to be the first to apply the method of Monte Carlo model to study the percolation threshold for disk-shaped fillers, simulating the conductive network formed by inclusions like graphene nanoplatelets. Later, Hicks et al. [17] developed a tunnelling-percolation model to investigate electrical transport in graphene-based nanocomposites, covering the need of a suitable model able to predict the full electrical response of semiconducting 2D element reinforced materials. This model, however, is applicable only to rectangle shaped nanoparticles forming 2D networks, while in common graphene reinforced nanocomposites, fillers exhibit a wide range of shapes, mainly circular-ellipsoid ones, and the conductive network formed is considered to be a 3D one. In simulation work [18], the percolation threshold for circular and ellipsoid fillers was investigated for a 2D network, while in [19] the percolation threshold of composites filled with intersecting circular disks and particles of various morphology was studied under a 3D Monte-Carlo simulation. Otten et al. [20] developed an analytical approach to investigate the percolation behaviour of polydisperse nanofillers, specifically focusing on the percolation threshold's sensitivity on the polydispersity in length, diameter and the level of conductivity of mainly needle-like filler nanocomposites. After the work of Hicks et al. [17] on the variation of electrical conductivity in respect of the volume fraction, Ambrosetti et al. [21] approached the electrical conductivity of an insulating matrix reinforced with conductive ellipsoids of revolution by assuming that an expected curve of electrical conductivity variation would be applied and finally being reduced in a geometrical form taking into account the inter-particle distance and the tunnelling distance. Mathew et al. [22] studied the percolation threshold of hard platelets in a 3D continuum system in terms of isotropic-nematic transition, while Hashemi et al. [23] proposed a continuum model developed, which embodied the most fundamental characteristics of the graphene nanocomposites (percolation threshold, interface effects and additional contribution of electron hopping, microcapacitor structures to interfacial properties) to determine the effective AC and DC electrical properties of graphene nanocomposites.

Knowing that, such numerical models are not easily applicable on industrial and engineering case study, as their employment is complicated and their results are limited to certain case, in this paper it is presented a multi-scale multi-physics finite element model (FEM) which would be easily applied to most cases, extended to more sophisticated material architecture in respect of being scientifically structured and proven. The current approach on multi scale modelling consists of the creation of a unit cell and a micro-scale nanocomposite model

(MSNM - Representative Volume Element RVE) on a commercial finite element modelling environment. The unit cell consists of a single rectangle graphene plate surrounded by a thin layer of polymer. This polymer layer represents the inter-plate volume between successive graphene reinforcements, in which conduction phenomena (tunnelling effect, electron hopping etc.) take place. The unit cell is loaded with a constant electric potential to compute the resistance matrix representing this system. The MSNM is a rectangle block, on whose resistance matrix elements previously obtained through the unit cell is randomly distributed. This distribution represents the random position of graphene on the bulk volume of polymer nanocomposites. The orientation of graphene is simulated by the 3D random orientation of the corresponding element local coordinate system.

2 FINITE ELEMENT MODELLING

2.1 Unit Cell

In similar terms with the approach of hard core-penetrable shell has been assumed on several studies predicting the percolation threshold [17], [24], the unit cell consists of a single-layer graphene plate surrounded by a thin layer of polymer. From this description, three main geometrical parameters could be derived-graphene's plate shape and size (expressed by the Aspect Ratio defined as the ratio of the length to the width) and the polymer layer thickness d_t. Graphene is modelled as an isotropic electrical conductive material with electrical conductivity of $\sigma=10^7$S/m, while the polymer layer represents the polymer volume between consecutive graphene, where the effect and the electron hoping phenomenon takes place. As a consequence, the conduction mechanism on polymer volume would be simulated by applying an exponentially varied resistivity ρ_{tunnel} expressed by the equation (1) in accordance to the findings of [25] for the electric tunnel effect between similar electrodes separated by a thin insulating film.

$$\rho_{tunnel} = \frac{h^2}{e^2\sqrt{2m\lambda}} \exp\left(\frac{4\pi d}{h}\sqrt{2m\lambda}\right) \qquad (1)$$

Since it has been assumed that the conductive phenomena taking place between two successive graphene plates would be taking into account in the unit cell analysis, it is necessary to modify the application of the tunnelling resistivity in the unit cell, so as to simulate the contribution of a single plate to the conduction. In many studies the cut-off distance, otherwise the maximum inter-particle distance above this the tunnelling effect is eliminated, was considered around 2 nm [17], [21], [26], leading to the polymer thickness range between 0 and 1.0 nm. In addition to this, it is crucial to note that the architecture of graphene plates forms conductive paths inside the insulating polymer, which could be represented as a typical 2D or even 3D resistor network. As a consequence, if the resistance of each unit cell was used to from a network, the result would be to add the resistance of two graphene plates and the tunnelling resistance assigned to each plate for every pair of plates. However, due to the fact that the tunnelling resistance is an exponential function of tunnelling distance, the sum of assigned tunnelling resistance of each plate would not be equal to the actual resistance. This observation implied the need to modify the equation (1) by multiplying it with the equation (2), so as to be able to simulate the actual tunnelling resistance when formed in a 3D real nanocomposite structure. In the proposed function (2), it is noticeable that the definition of the tunnelling resistivity applied on the unit cell would not be a deterministic variable but a stochastic one. This statistical feature, then, should be transferred to the next scale and be applied on the representative volume implying complicated distributions on material properties. In order to

eliminate this effect, it is proposed to use an equivalent constant C in combination with the modified equation (3) of tunnelling resistivity. The constant C would be given by the equation (4), depicted in Figure 1 and its equivalent value would be the result of the equation (5). The equivalent value of C for each case is presented in Table 2, where it is possible to conclude that assuming C being equal to 0.3 would be reasonable to represent each case.

$$\frac{R_{tunnel}(d_1+d_2)}{R_{tunnel}(d_1)+R_{tunnel}(d_2)}=\frac{d_1}{d_1+d_2}\exp\left(\frac{-4\pi d_2}{h}\sqrt{2m\lambda}\right)+\frac{d_2}{d_1+d_2}\exp\left(\frac{-4\pi d_1}{h}\sqrt{2m\lambda}\right) \quad (2)$$

$$\rho_{tunnel}=C_{equivalent}\frac{h^2}{e^2\sqrt{2m\lambda}}\exp\left(\frac{8\pi d}{h}\sqrt{2m\lambda}\right) \quad (3)$$

$$R_{tunnel}(d_1+d_2)=C\left(R_{tunnel}(d_1)\exp\left(\frac{4\pi d_1}{h}\sqrt{2m\lambda}\right)+R_{tunnel}(d_2)\exp\left(\frac{4\pi d_2}{h}\sqrt{2m\lambda}\right)\right) \quad (4)$$

$$C_{equivalent}(d_{\max}-d_{\min})=\int_{d_{\min}}^{d_{\max}}C(\delta)d\delta \quad (5)$$

Plank's constant	h	m^2kg/s	$6.62607004\cdot10^{-34}$
Electron charge	e	Coulomb	$1.60217662\cdot10^{-19}$
Electron mass	m	kg	$9.10938356\cdot10^{-31}$
Height of barrier	λ	eV	0.5-2.5
Polymer layer thickness/Tunnelling distance	d_t	nm	0.0-1.0

Table 1: Tunnelling resistivity variables and parameters

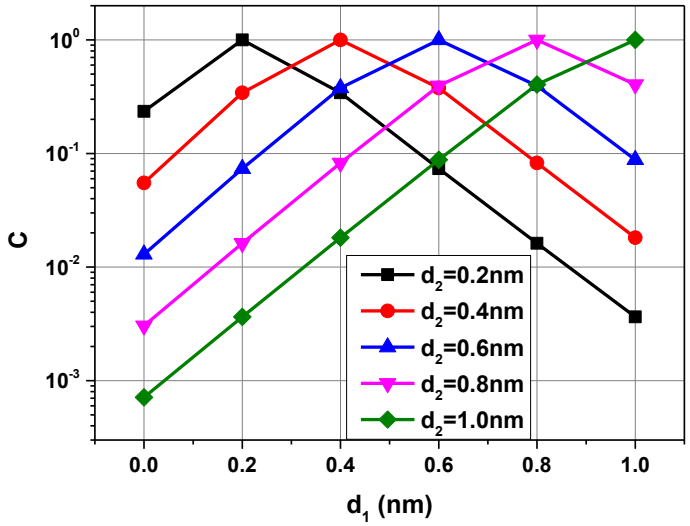

Figure 1: Variation of constant C in function of polymer thickness surrounding graphene layer.

d_2 (nm)	$C_{equivalent}$
0.2	0.37
0.4	0.37
0.6	0.38
0.8	0.34
1.0	0.20

Table 2: $C_{equivalent}$ in function of d_2.

In terms of finite element analysis, the proposed model was built in commercial FEA program ANSYS 16.2. A 3D 20-Node Hex couple-field solid element was used with its piezoresistive behaviour activated through the available key-option 101, while both for graphene and polymer isotropic electrical behaviour was assumed. It is important to mention that the piezoresistive coupling induced by this key-option was neglected by not defining the piezoresistive matrix. The values of the parameters used on the analysis of the unit cell are presented on the Table 3 and Table 4. Unit cell is loaded in the longitudinal, transverse and through thickness direction by a constant voltage, simulating DC loading and resulting to the calculation of the resistance matrix by the use of Ohm's law.

Graphene Shape		Rectangular	Ellipse
Graphene plate thickness	t (nm)	0.45	0.45
Graphene minor side dimension	a (nm)	10	2·5.64
Aspect Ratio	AR (-)	1,5,10,50	1,2,5,7,10
Graphene major side dimension	b (nm)	AR·a	AR·a

Table 3: Graphene geometrical parameters

Material	Electrical behaviour		
Graphene	Electrical conductivity	S/m	10^7
Polymer	Tunnelling resistivity	Ωm	Equation (3)
	$C_{equivalent}$	-	0.3
	Height of barrier (λ)	eV	0.5-2.5
	Tunnelling distance (d)	nm	0.2-1.0

Table 4: Unit cell material properties

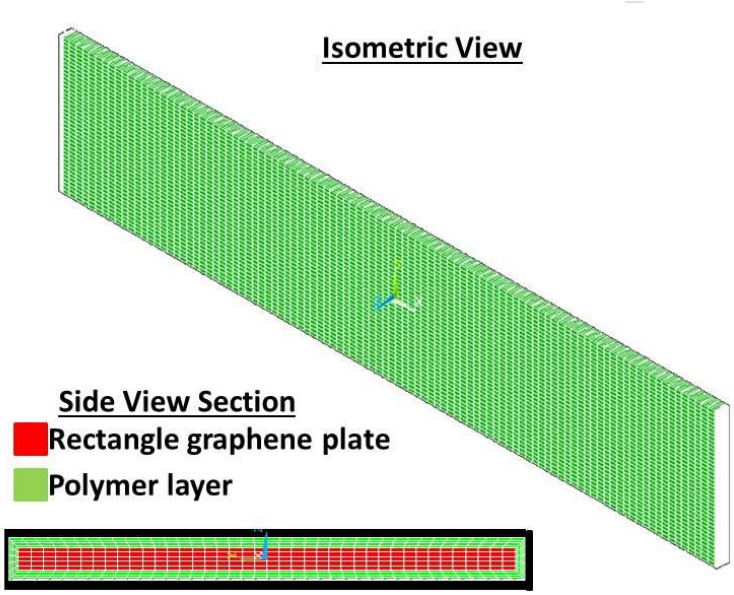

Figure 2: Unit Cell finite element model.

2.2 Representative Volume Element (RVE)

The nanocomposite structure was approached by a square block of side equal to multiplied b (k·b) and thickness of multiplied a (k·a). The number of graphene seeds on the block is defined by equations (6) and (7) as a function of nanocomposites volume fraction and graphene's geometry. The number of elements representing each graphene layer (γ) would equal to the number of division in the direction of loading (eix) divided by the factor k. As a consequence the number of elements representing graphene reinforcement in total in the volume (n_g) would be given by the equation (8). The number of elements in the perpendicular to loading direction (eiz) would be given by the equations (9) and (10), while the number of elements through the block's thickness (eiy) would be eiz/AR.

Number of graphene seeds in respect of the graphene shape		
Square - Rectangle	$n = V_f \frac{k^3 ARa}{t}$	(6)
Circle - Ellipse	$n = V_f \frac{k^3 ARa}{\pi t}$	(7)

Table 5: Equations describing the number of graphene seeds in respect of the graphene shape.

$$n_g = \gamma n = n\frac{eix}{k} \quad (8)$$

Number of element on perpendicular to loading direction in respect of graphene shape		
Square - Rectangle	$eiz = kAR\sqrt{\frac{a}{t}}$	(9)
Circle - Ellipse	$eiz = kAR\sqrt{\frac{a}{\pi t}}$	(10)

Table 6: Equations describing the number of elements on perpendicular to loading direction in respect of the graphene shape.

The nanocomposite's architecture is approached by the distribution of the graphene plates being enforced by choosing n_g non-repeatable integer numbers. Each number indicates the element ID number in the FE model. Each selected element has the electrical properties resulted by the analysis of the unit cell. Especially, assuming DC linear electrical behaviour, the electrical response of the unit cell in each element is introduced in accordance to equations presented in Table 7. The tunnelling distance between two successive graphene particles is assigned by random choice of material types obtained by unit cell and related to a specific tunnelling distance. Finally, the orientation of graphene layers in the volume is approached by the orientation of the element local coordinate system with rotation angles of $THXY \in [0,90]$, $THZY \in [0,90]$ and $THXZ \in [0,90]$. The elements, which have not been chosen to represent graphene sheets, are simulated as pure insulating matrix with electrical resistivity of $10^{16}\Omega$m. The RVE model was built up under the same principles as the unit cell one. The volume is loaded with constant voltage, while the result of the analysis is the reaction current. With the use of the Ohm's law and under the conduction of 50 separate analysis per case, the variation of electrical conductivity in respect of volume fraction is created, while in the probability function of percolation the inflection point is calculated to be the percolation threshold in accordance to the suggested procedure of [22].

Electrical resistivity distributed in the RVE in respect of the direction		
x-axis	$\rho_x = R_x^{unitcell} \frac{k^2 ARa}{eiz^2}$	(11)
y-axis	$\rho_y = R_y^{unitcell} \frac{k^2 ARa}{eix^2}$	(12)
z-axis	$\rho_z = R_z^{unitcell} \frac{k^2 ARa}{eix^2}$	(13)

Table 7: Equations for the electrical resistivity introduced to the elements representing graphene particles in respect of the direction.

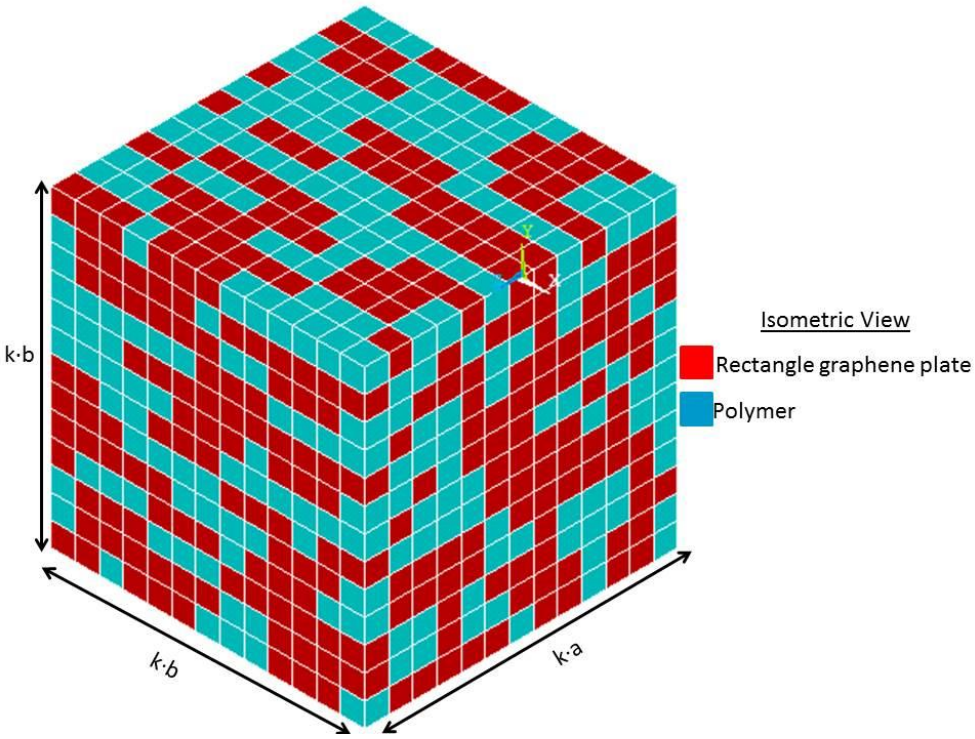

Figure 3: Representative Volume Element finite element model.

3 RESULTS

3.1 Unit cell analysis

After the analysis of the unit cell in respect of all the parameters mentioned on Table 3 and Table 4, it is possible to make some notes on the effect of these feature on the unit cell resistance, which could be assumed to represent the local resistance shown on a nanocomposite structure. As far as the effect of the aspect ratio is concerned, in Figure 4 this effect is depicted in respect of the loading direction and tunnelling distance for rectangle shaped graphene and height of barrier of 0.5eV. It could be noted that the rise of the aspect ratio leads to significant decrease in the resistance, as the resistance of the graphene has been the dominant conduction mean in the unit cell. Especially in the case of aspect ratio being greater than 50, in the longitudinal direction of the unit cell (x-direction) the resistance saturates to a constant value in function of the tunnelling distance.

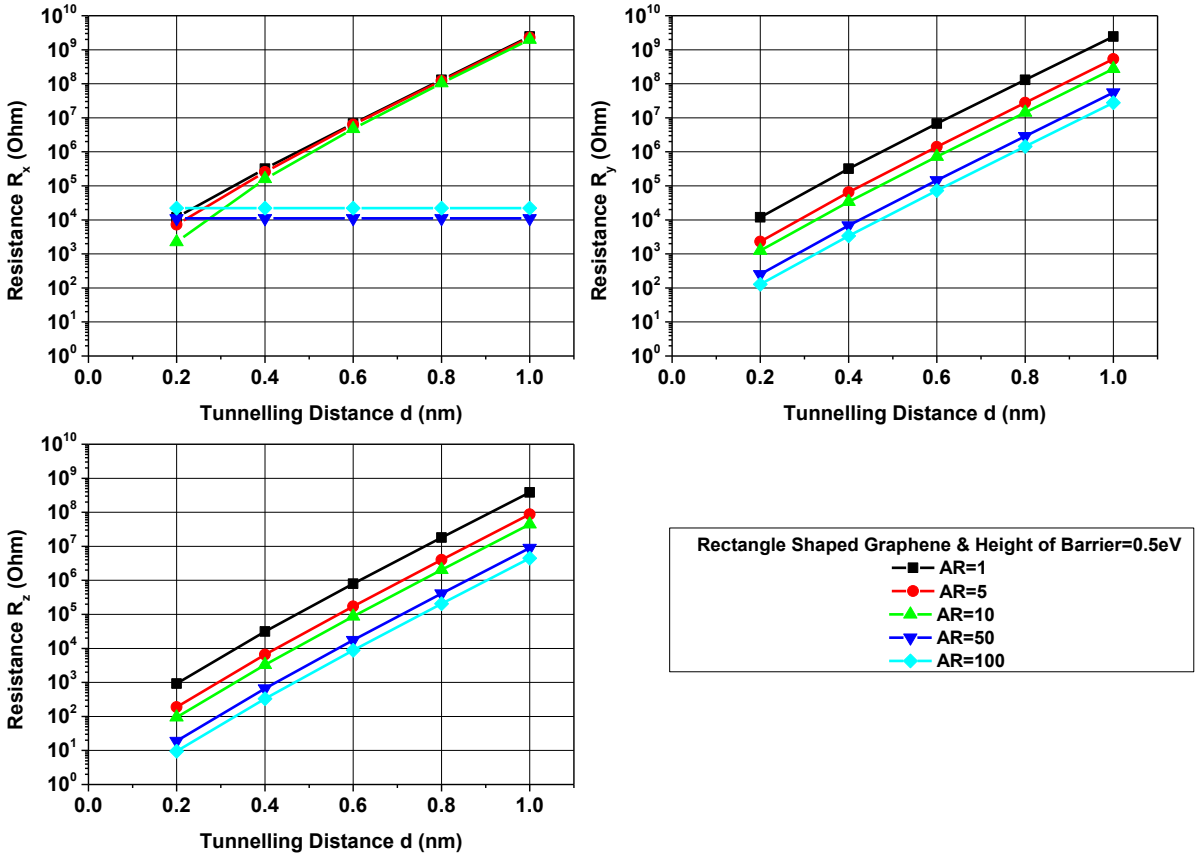

Figure 4: Effect of aspect ratio on unit cell resistance for the case of rectangular shaped graphene and height of barrier of 0.5eV in respect of the direction and the tunnelling resistance.

Polymer and all the features controlling its response under any excitation (degree of polymerization, voids, humidity, temperature etc.) have serious effect on the electrical conductivity of a nanocomposite through the energy quantity of height of barrier appearing on the tunnelling resistivity. As it is thoroughly explained in [25], when two conductive particles are separated by an insulating film (polymer film in this case), the equilibrium conditions require that the top of the energy gap of the insulator to be positioned above the Fermi level of the conductive particles. As a result, the action of the insulating film is to introduce a potential barrier between the electrodes which impedes the flow of the electron between the conductive particles. This description of the physical system of conductive particles separated by an insulator suggests that electronic current would flow through the insulating region between the conductive particles if the electron had enough thermal energy to overcome the potential barrier and flow in the conduction band or even if the barrier was that low to permit its penetration by the electric tunnel effect. This potential barrier is described in this study as height of barrier and usually takes values of a few electron volts (0.5-2.5eV). In this part of our study, the effect of height barrier on the unit cell resistance in respect of tunnelling distance and for the case of rectangle shaped graphene with aspect ratio of 1 and 5 is depicted in Figure 5. The rise of the height of barrier has as a consequence the rise of the local resistance even in orders of magnitude. This increasing trend is common for every case of unit cell studied, while becomes more evident with the increase of tunnelling distance.

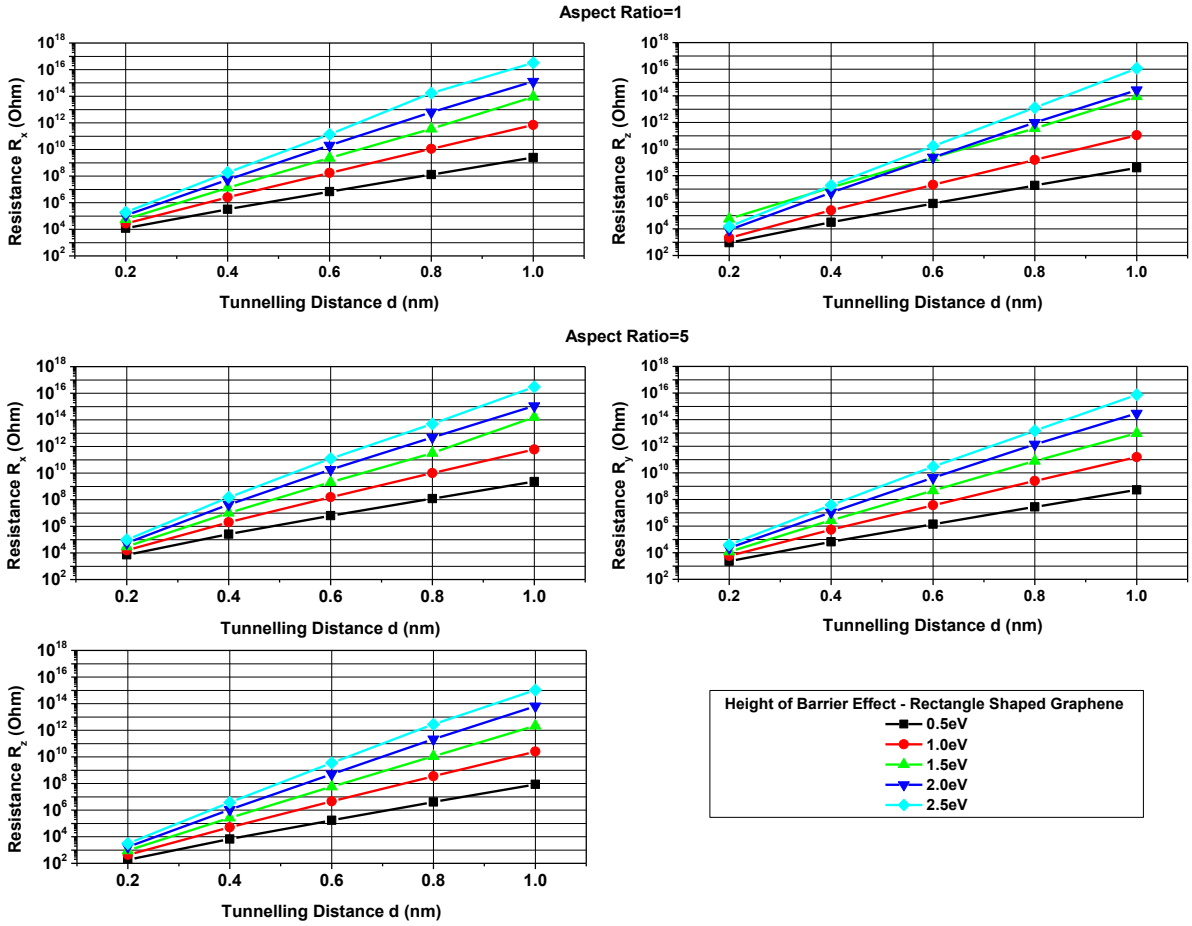

Figure 5: Effect of height of barrier on unit cell resistance for the case of rectangular shaped graphene filler and aspect ratio of 1 & 5 in respect of the direction and the tunnelling resistance.

Finally, the shape of the graphene layer is considered. In Figure 6, the effect of graphene shape on the unit cell resistance in respect of the direction and the tunnelling distance is depicted for all examined aspect ratios and height of barrier of 0.5eV. It could be stated that ellipse shaped graphene sheets exhibit higher local resistance in the main axis directions than the rectangle shaped ones. However, for the case of the through thickness resistance, for the common aspect ratios ellipse and rectangle shaped graphene plates show the same electrical resistance. It is important to mention that for the purposes of comparison, the area of the rectangle shaped graphene layers is equal to that of the elliptical shaped graphene layers for each aspect ratio.

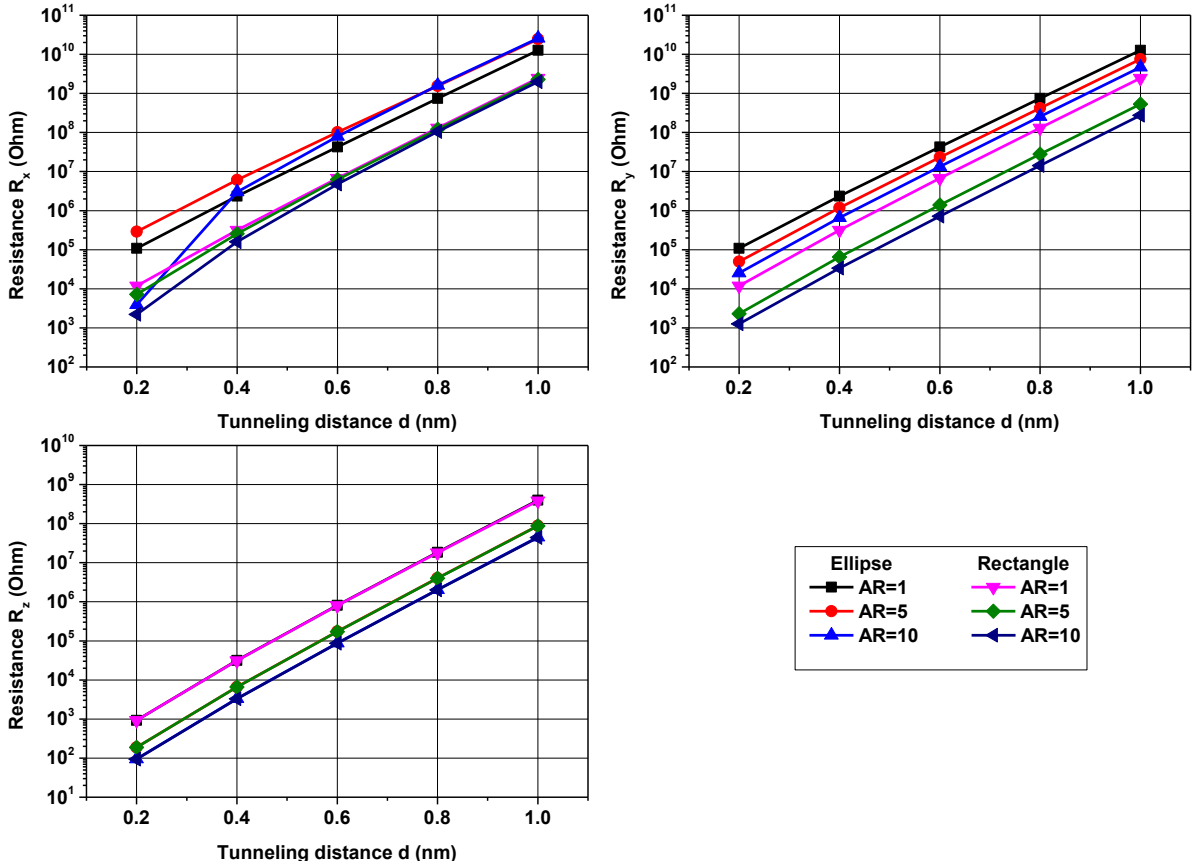

Figure 6: Effect of graphene shape on the unit cell resistance for all examined aspect ratios, height of barrier of 0.5eV in respect of the direction and the tunnelling resistance.

3.2 RVE analysis

Since it is not reasonable to model infinite material and in order to eliminate the edge effect, it is important to conduct a convergence study on the size of the square block. Having considered as value identical to the nanocomposite structure the ratio of the average of the electrical conductivity of the sample to its standard deviation, as it could be noticed in the Figure 7, for k=5 the structure of the nanocomposite has converged.

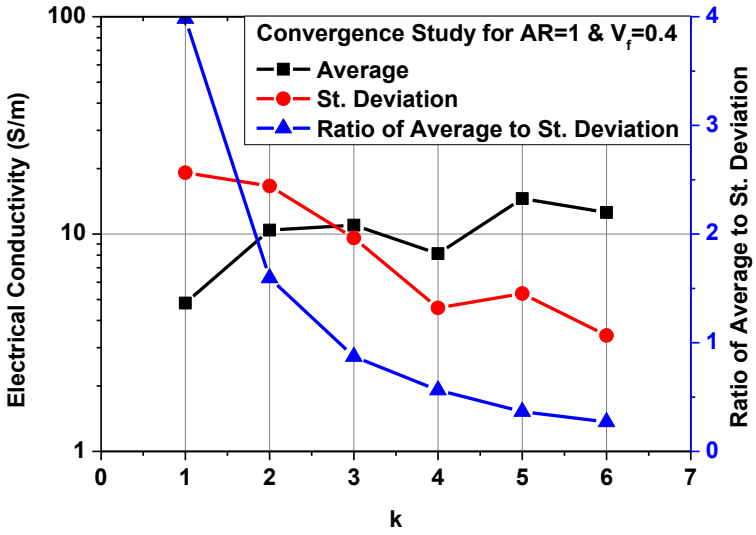

Figure 7: Convergence study on the size of the representative volume for the case of the graphene filler with aspect ratio=1 and V_f=0.4.

As it has been already stated the percolation probability, in accordance to the procedure suggested by the [22], is fitted by the function (14) and the inflection point of this function is considered to be the percolation threshold. In Figure 8, the percolation probability in respect of the volume fraction is depicted for the case of rectangle graphene sheets and λ=0.5eV. As it could be noted, the proposed fitting function is suitable for describing this kind of data set achieving 99.999% accuracy on fitting process.

$$P(V_f) = \frac{1}{2}\left(1 + \tanh\left(A\left(V_f - B\right)\right)\right) \qquad (14)$$

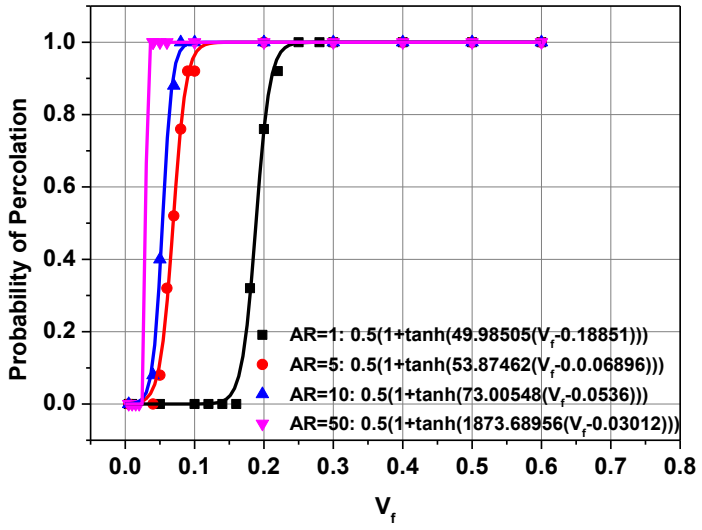

Figure 8: Percolation probability in respect of volume fraction for studied graphene aspect ratios for the case of λ=0.5eV and the corresponding functions.

In Figure 9, the effect of aspect ratio on the variation of electrical conductivity in respect of the graphene volume fraction for the case of rectangle shaped filler. It is notable that, the rise in aspect ratio leads to decrease on the volume fraction on which the onset of conductance occurs. In addition to this, for a constant value of volume fraction, nanocomposite's electrical conductivity increases with rising aspect ratio. These results suggest that fillers with high aspect ratio are able to form more stable and efficient conductive network in the volume of nanocomposite in lower volume fraction. The above conclusion is supported also by the fact that with the rise of volume fraction the deviation on the statistical sample is significantly reduced leading to more uniform sample close to uniquely defined electrical conductivity for a nanocomposite of a specific volume fraction.

In Figure 10, the effect of height of barrier on nanocomposite's electrical conductivity is depicted for the case of rectangle shaped graphene with aspect ratio equal to 1 and 5. Although, the percolation threshold seems no to be affected by the height of barrier, since the onset of percolation is mainly geometrically oriented as it has been proven by [23], for the case of constant volume fraction the rise of height of barrier causes rapid decrease on the nanocomposite's electrical conductivity even by a decrease of an order of magnitude in the case of increasing the height of barrier by 0.5eV.

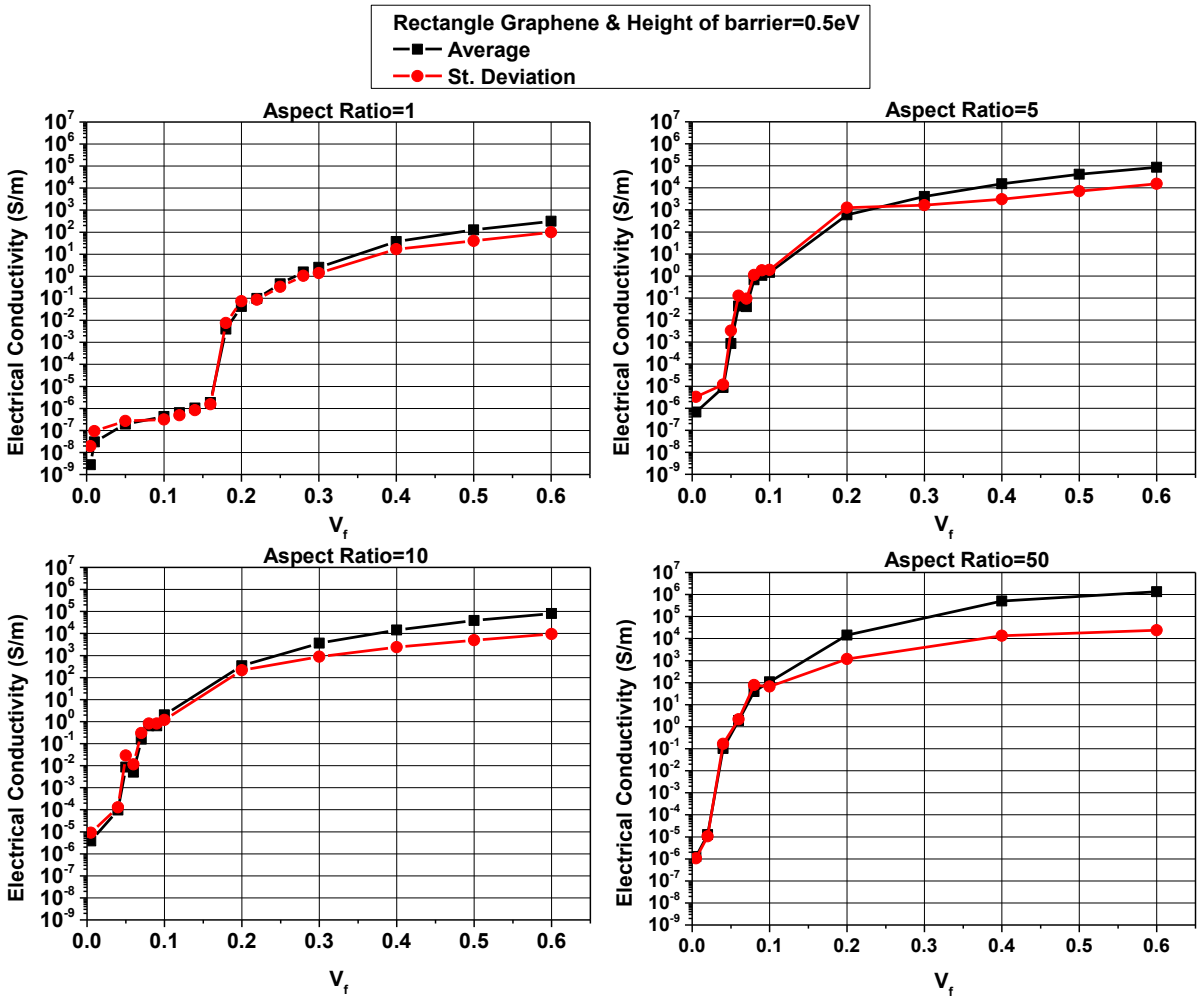

Figure 9: Effect of aspect ratio on the electrical conductivity in respect of volume fraction V_f for rectangle shaped graphene and height of barrier λ=0.5eV.

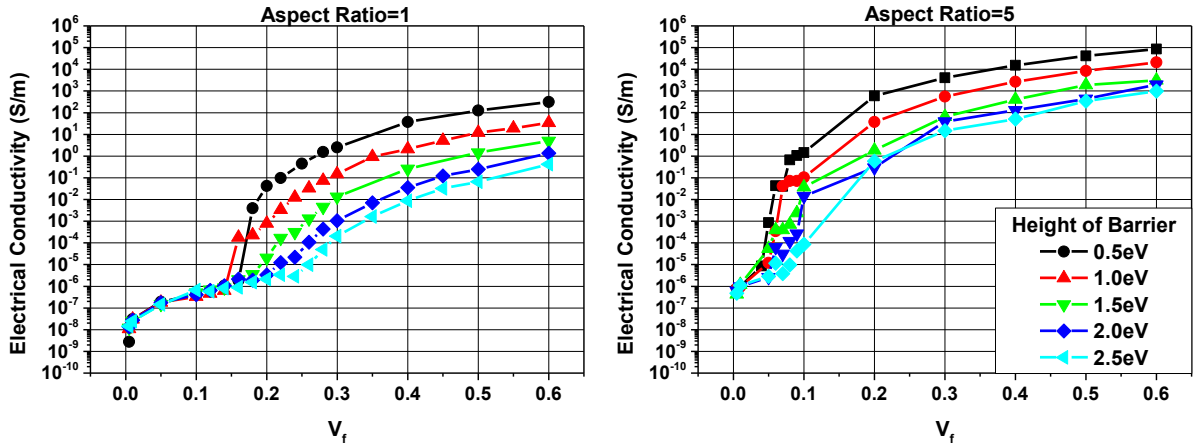

Figure 10: Effect of height of barrier on the electrical conductivity in respect of volume fraction V_f for rectangle shaped graphene and aspect ratios of 1 &5.

In Figure 11 the effect of the graphene shape is depicted in respect of the volume fraction for the case of height of barrier being 0.5eV. The graphene shape does not affect the trend of the nanocomposite electrical response in function of the V_f, although for graphene particles of the same aspect ratio and volume, the nanocomposite reinforced with rectangle shaped exhibits higher electrical conductivity than that of a nanocomposite reinforced with ellipse shaped graphene particles, while the rectangle shaped graphene particles show lower percolation threshold than that obtained for the ellipse graphene. [27] suggested that this observation could be explained as the corner angles of squares and rectangles make it easier for the plates to touch each other, therefore enhancing the current passing from the one particle to another.

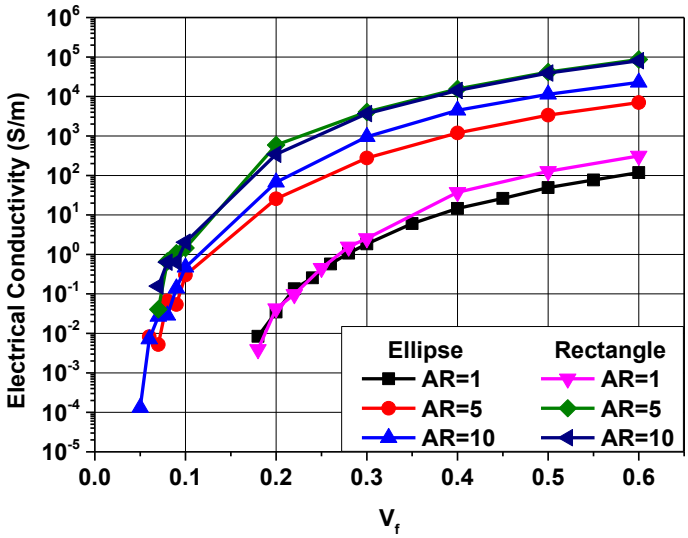

Figure 11: Effect of graphene shape on the electrical conductivity in respect of the volume fraction V_f for height of barrier of 0.5eV.

3.3 Percolation model

For the description of the percolation behaviour of the nanocomposites, several theories have been suggested with more popular the percolation law, which describes the variation of

the electrical conductivity of the nanocomposite in respect of the volume fraction after the percolation threshold having being obtained, and the excluded volume theory, which is able to predict the percolation threshold of a nanocomposite in respect of the geometrical features of the reinforcement (dimensions, shape, 2D-3D conductive networks).

Taking into consideration the excluded volume theory and assuming that the each particle could be considered equivalent to a circular one, the excluded volume theory for the circular disk [28] could be modified so as to define the upper and lower boundaries of the volume fraction in which the percolation threshold should be expected (15). In Figure 12, it could be obvious that the percolation threshold is reduced with increasing aspect ratio, the values were successfully found to lie between the assumed percolation bounds. In addition to this, the shape of the graphene seems not to show any effect on the percolation threshold, since the corresponding values for each case are in good agreement.

$$\left.\begin{array}{l} 1-\exp\left(-1.4\dfrac{V}{V_{ex}}\right) \le V_c \le 1-\exp\left(-2.8\dfrac{V}{V_{ex}}\right) \\ V=\pi\left(\dfrac{d}{2}\right)^2 t \\ V_{ex}=\pi^2\left(\dfrac{d}{2}\right)^3 \end{array}\right\} \xrightarrow{\frac{d}{2}=\alpha\sqrt{\frac{AR}{\pi}}} 1-\exp\left(-1.4t\frac{\sqrt{\pi}}{\alpha\sqrt{AR}}\right) \le V_c \le 1-\exp\left(-2.8t\frac{\sqrt{\pi}}{\alpha\sqrt{AR}}\right) \quad (15)$$

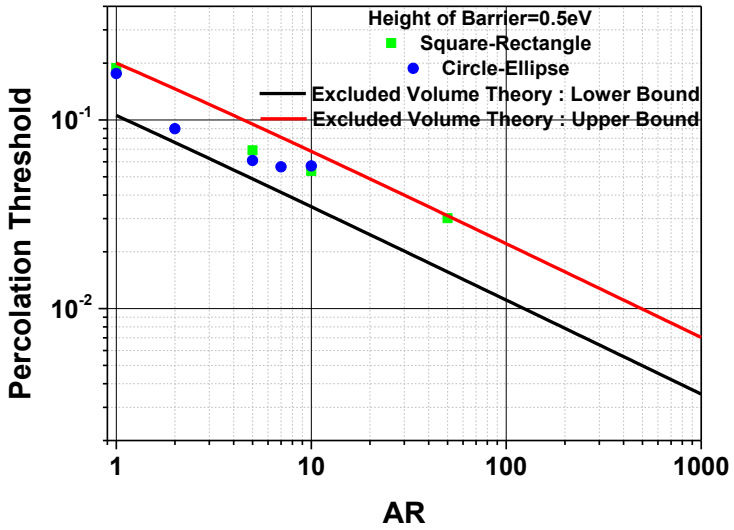

Figure 12: Percolation Threshold in respect of the graphene shape and boundary functions (15).

The percolation law is a power equation (16) introduced in [29], which is able to describe to electrical behaviour of an insulating material reinforced with conductive particles after the percolation threshold. In the equation (16) σ_c is the electrical conductivity of the composite, V_f is the volume fraction, V_p is the percolation threshold, σ_o is a factor with value close the electrical conductivity of the conductive phase measured in units of electrical conductivity and t is the critical exponent. For a three dimensional conductive network, t usually takes value between 1.65 and 2.0, which is accepted as a universal value. Higher values of t indicate

the presence of tunnelling phenomena and the filler having extreme geometries (i.e. high aspect ratio). In Figure 13, the fitting of the finite element model results in accordance to the percolation law is presented, showing a good correlation, while in Figure 14 the effect of the geometry of the filler and the height of barrier on the percolation law variables is depicted. As far as the σ_o is concerned, it is increased with rising aspect ratio converging to the filler electrical conductivity, while it is fallen with increasing height of barrier. The increase on aspect ratio leads to more stable electrical networks which are mainly governed by the fillers conductance and not the tunnelling resistance formed in the interparticle region, leading σ_o to converge to the electrical conductivity of the filler. On the other hand, the rise of height of barrier which induces a rise on the tunnelling resistance in the interparticle volume, has as a consequence the decrease of the σ_o for the case of low aspect ratios. One of the most significant findings related to the percolation law is the agreement of the observation to the general law regarding the critical exponent. An increase on the aspect ratio (defining an extreme geometry) or even any rise of the height of barrier (defining a more intense tunnelling phenomenon) has a result an important increase of the value of the critical exponent far above the prediction for a common three dimensional conductive network.

$$\sigma_c = \sigma_o \left(V_f - V_p\right)^t \tag{16}$$

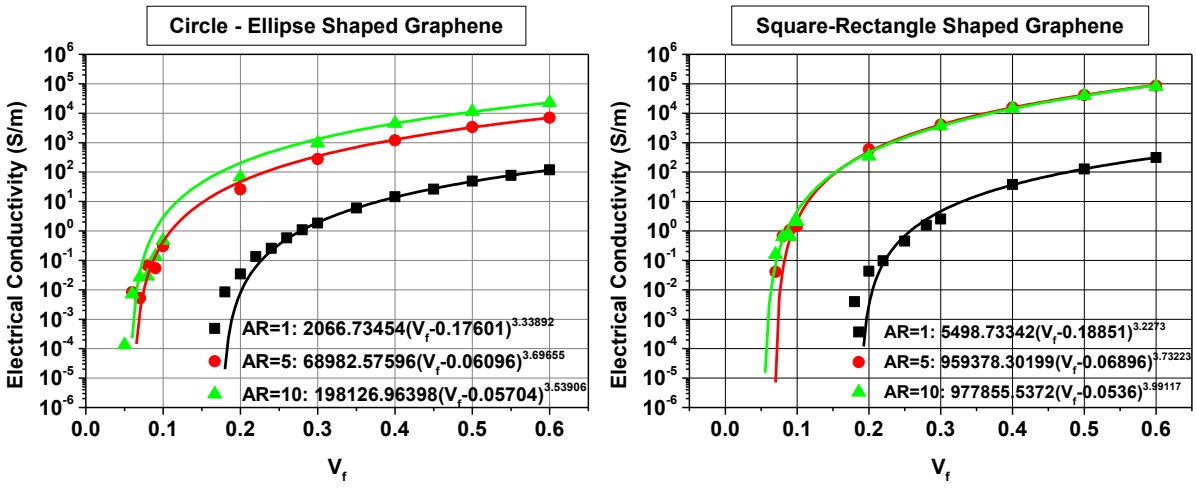

Figure 13: Percolation Law in respect of the aspect ratio and the shape of the graphene particle for the case of height of barrier of 0.5eV.

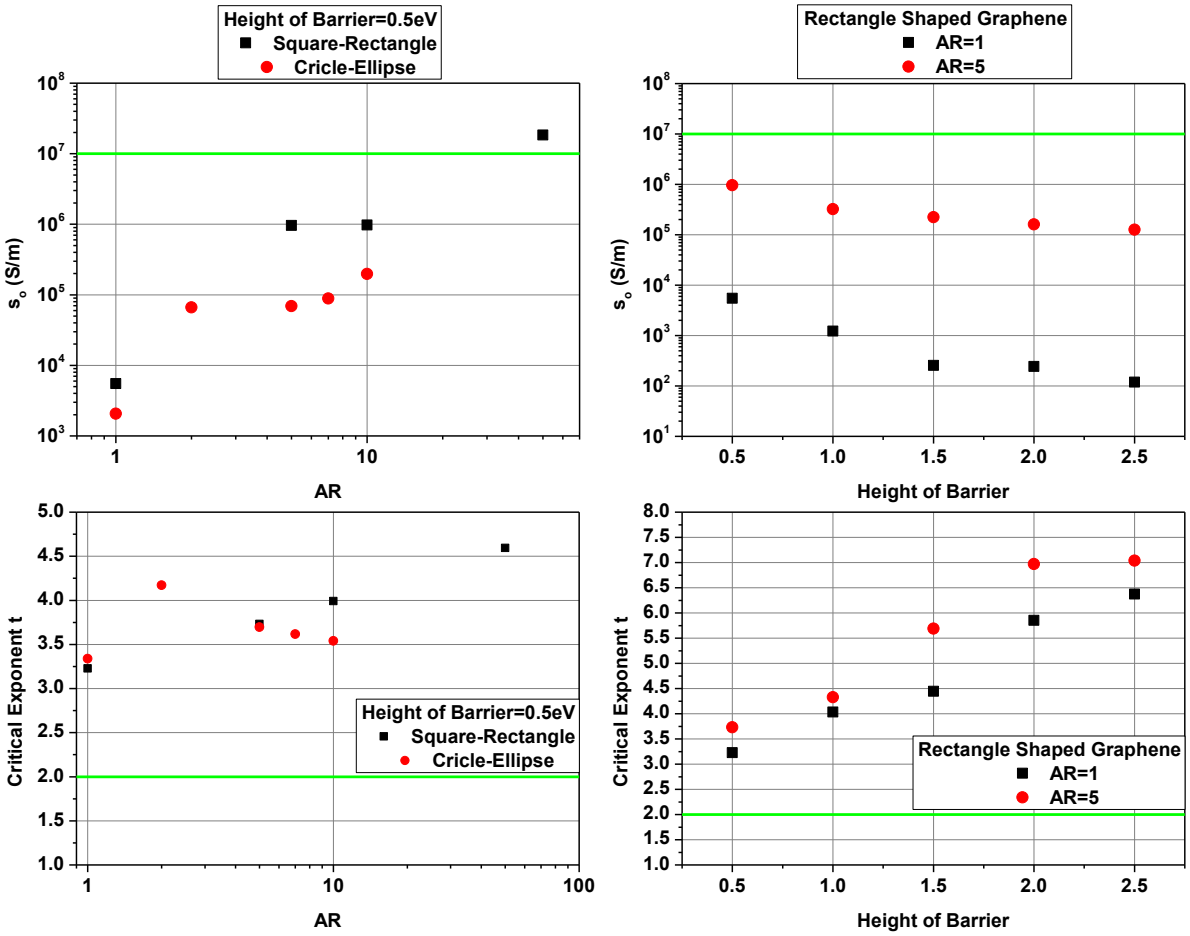

Figure 14: Variation of the percolation law variables in respect of the aspect ratio, the shape of graphene and the height of barrier.

4 CONCLUDING REMARKS

- The finite element model has been shown to effectively simulate the electrical response of the selected graphene/polymer composite under DC loading.
- The results are in accordance to theoretical predictions.
- Increasing the Aspect Ratio reduces the percolation threshold and increases the electrical conductivity of the nanocomposite for a given value of volume fraction.
- The tunnelling resistance exhibited in the inter-particle volume affects the overall performance of the nanocomposite, especially due to the height of barrier, whose rise increases the inter-particle resistance and decreases the electrical conductivity of the nanocomposite.
- The shape of the graphene fillers do not show any significant effect in terms of percolation, but the formation of sufficient contact between particles for the charge transfer is enhanced for the case of rectangular shaped graphene.

REFERENCES

[1] E. K. Sichel, J. I. Gittleman, and P. Sheng, "Electrical properties of carbon-polymer composites," *J. Electron. Mater.*, vol. 11, no. 4, pp. 699–747, Jul. 1982.

[2] Y. Ishigure, S. Iijima, H. Ito, T. Ota, H. Unuma, M. Takahashi, Y. Hikichi, and H. Suzuki, "Electrical and elastic properties of conductor-polymer composites," *J. Mater. Sci.*, vol. 34, no. 12, pp. 2979–2985.

[3] G. Pinto and A. Jiménez-Martín, "Conducting aluminum-filled nylon 6 composites," *Polym. Compos.*, vol. 22, no. 1, pp. 65–70, Feb. 2001.

[4] V. . Roldughin and V. . Vysotskii, "Percolation properties of metal-filled polymer films, structure and mechanisms of conductivity," *Prog. Org. Coatings*, vol. 39, no. 2–4, pp. 81–100, Nov. 2000.

[5] L. Flandin, J. Y. Cavaillé, G. Bidan, and Y. Brechet, "New nanocomposite materials made of an insulating matrix and conducting fillers: Processing and properties," *Polym. Compos.*, vol. 21, no. 2, pp. 165–174, Apr. 2000.

[6] S. S. Ray and M. Biswas, "Water-dispersible conducting nanocomposites of polyaniline and poly(N-vinylcarbazole) with nanodimensional zirconium dioxide," *Synth. Met.*, vol. 108, no. 3, pp. 231–236, Feb. 2000.

[7] A. Quivy, R. Deltour, A. G. M. Jansen, and P. Wyder, "Transport phenomena in polymer-graphite composite materials," *Phys. Rev. B*, vol. 39, no. 2, pp. 1026–1030, Jan. 1989.

[8] W. Zheng, S.-C. Wong, and H.-J. Sue, "Transport behavior of PMMA/expanded graphite nanocomposites," *Polymer (Guildf).*, vol. 73, pp. 6767–6773, 2002.

[9] W. Zheng and S.-C. Wong, "Electrical conductivity and dielectric properties of PMMA/expanded graphite composites," *Compos. Sci. Technol.*, vol. 63, pp. 225–235, 2003.

[10] G. Chen, W. Weng, D. Wu, and C. Wu, "PMMA/graphite nanosheets composite and its conducting properties," *Eur. Polym. J.*, vol. 39, pp. 2329–2335, 2003.

[11] H. Kim, Y. Miura, and C. W. Macosko, "Graphene/Polyurethane Nanocomposites for Improved Gas Barrier and Electrical Conductivity," *Chem. Mater*, vol. 22, pp. 3441–3450, 2010.

[12] Y. Song, J. Yu, L. Yu, F. E. Alam, W. Dai, C. Li, and N. Jiang, "Enhancing the thermal, electrical, and mechanical properties of silicone rubber by addition of graphene nanoplatelets," *JMADE*, vol. 88, pp. 950–957, 2015.

[13] C. Yun, Y. Feng, T. Qiu, J. Yang, X. Li, and L. Yu, "Mechanical, electrical, and thermal properties of graphene nanosheet/aluminum nitride composites," *Ceram. Int.*, vol. 41, pp. 8643–8649, 2015.

[14] M. H. Al-Saleh, "Electrical and mechanical properties of graphene/carbon nanotube hybrid nanocomposites," *Synth. Met.*, vol. 209, pp. 41–46, 2015.

[15] E. Kandare, A. A. Khatibi, S. Yoo, R. Wang, J. Ma, P. Olivier, N. Gleizes, and C. H. Wang, "Improving the through-thickness thermal and electrical conductivity of carbon fibre/epoxy laminates by exploiting synergy between graphene and silver nanoinclusions," *Compos. PART A*, vol. 69, pp. 72–82, 2015.

[16] A. B. Oskouyi and P. Mertiny, "Monte Carlo model for the study of percolation thresholds in composites filled with circular conductive nano-disks," *Procedia Eng.*, vol. 10, pp. 403–408, 2011.

[17] J. Hicks, A. Behnam, and A. Ural, "A computational study of tunneling-percolation electrical transport in graphene-based nanocomposites," *Appl. Phys. Lett.*, vol. 95, no. 21, pp. 213103:1–213103:3, 2009.

[18] W. Xia and M. F. Thorpe, “Percolation properties of random ellipses,” *Phys. Rev. A*, vol. 38, no. 5, pp. 2650–2656, Sep. 1988.
[19] L. Vovchenko and V. Vovchenko, “Simulation of percolation threshold in composites filled with conducting particles of various morphologies,” *Materwiss. Werksttech.*, vol. 42, no. 1, pp. 70–74, Jan. 2011.
[20] R. H. J. Otten and P. Van Der Schoot, “Connectivity percolation of polydisperse anistropic nanofillers,” *J. Chem. Phys.*, vol. 134, pp. 094902:1–094902:15, 2011.
[21] G. Ambrosetti, C. Grimaldi, I. Balberg, T. Maeder, A. Danani, and P. Ryser, “Solution of the tunneling-percolation problem in the nanocomposite regime,” *Phys. Rev. B*, vol. 81, no. 15, p. 155434, Apr. 2010.
[22] M. Mathew, T. Schilling, and M. Oettel, “Connectivity percolation in suspensions of hard platelets.,” *Phys. Rev. E. Stat. Nonlin. Soft Matter Phys.*, vol. 85, no. 6 Pt 1, p. 061407, Jun. 2012.
[23] R. Hashemi and G. J. Weng, “A theoretical treatment of graphene nanocomposites with percolation threshold, tunneling-assisted conductivity and microcapacitor effect in AC and DC electrical settings,” *Carbon N. Y.*, 2016.
[24] G. Ambrosetti, N. Johner, C. Grimaldi, A. Danani, and P. Ryser, “Percolative properties of hard oblate ellipsoids of revolution with a soft shell,” *Phys. Rev. E*, vol. 78, pp. 061126:1–061126:11, 2008.
[25] J. G. Simmons, “Generalized Formula for the Electric Tunnel Effect between Similar Electrodes Separated by a Thin Insulating Film,” *J. Apllied Phys.*, vol. 34, no. 6, pp. 1793–1803, 1963.
[26] A. B. Oskouyi, U. Sundararaj, and P. Mertiny, “Tunneling Conductivity and Piezoresistivity of Composites Containing Randomly Dispersed Conductive Nano-Platelets,” *Materials (Basel).*, vol. 7, pp. 2501–2521, 2014.
[27] Y. B. Yi and E. Tawerghi, “Geometric percolation thresholds of interpenetrating plates in three-dimensional space,” *Phys. Rev. E*, vol. 79, no. 04, pp. 041134:1–041134:6, 2009.
[28] I. Balberg, C. H. Anderson, S. Alexander, and N. Wagner, “Excluded volume and its relation to the onset of percolation,” *Phys. Rev. B*, vol. 30, no. 7, pp. 3933–3943, 1984.
[29] D. Stauffer and A. Aharony, *Introduction to Percolation Theory*, Revised Se. London: Taylor & Francis, 1994.